



ISSN: 0067-2904

Comprehensive Analysis of Pair Galaxy UGC 8335 Using Multiple Filters

Haydar R. Al-baqir*, Abdullah K. Ahmed

Astronomy and Space Department, College of Science, University of Baghdad, Baghdad, Iraq

Received: 3/11/2023 Accepted: 2/9/2024 Published: 15/11/2024

Abstract

The two galaxies, UGC 8335 (East) E and (West) W, were investigated through the utilization of photometric and spectroscopic approaches, employing g, r, i, and z filters to gather the maximum amount of details feasible; the observed data were obtained using the data releases (DR7 and DR17) provided by "The Sloan Digital Sky Survey (SDSS)." Subsequently, the data were fitted to ellipsoids through the utilization of "the Images Reduction & Analysis Facilities (IRAF)" through implementation of the STSDAS ELLIPS tool. Multiple characteristics of the two galaxies UGC 8335 E and W, have been scrutinized, including surface brightness, magnitudes, both vertical and horizontal changes, accumulated flux, central axis position angles, ellipticities, isophotal shape parameters (B4), and star-forming rates (SFRs), together with their astronomical characteristics. The UGC 8335 galaxy pair has been confirmed to be an interacting pair that exhibits significant indications of interaction and is undergoing a merging process. Furthermore, this combination is categorized as an intermediate galaxy pair and represents a physical set with refined star formation rates.

Keywords: Interacting galaxy, merging galaxy, UGC 8335 E, UGC 8335 W, spectroscopy, and surface photometry, SDSS Filters.

تحليل شامل للزوج المجري UGC 8335 باستخدام فلاتر متعددة

حيدر رضا حسين الباقير*, عبد الله كامل احمد

قسم الفلك والفضاء ، كلية العلوم ، جامعة بغداد ، بغداد ، العراق

الخلاصة

تمت دراسة المجرتين UGC 8335 E و W ، من خلال باستخدام طرق القياس الضوئي والطيفي باستعمال فلاتر g, r, i, z وجمع اكبر قدر ممكن من التفاصيل. البيانات الرصدية اخذت من اصدارات Sloan Digital Sky Survey " (DR7 and DR17) المقدمة من " (SDSS) ، وبعد ذلك تم عمل ال fitting للبيانات باستخدام برنامج (IRAF) من خلال المكتبة STSDAS تحديدا ELLIPS task. تم فحص خصائص متعددة للمجرتين UGC 8335 E و W بما في ذلك كل من اللمعان السطحي ، الاقدار ، الانحرافات العمودية والأفقية ، الانبعث الكلي ، وزوايا انحراف المحور الكبير ، وشكل القطع الناقص ، الانحرافات العمودية والأفقية ، ومعاملات كيرشوف للشكل (B4)، ومعدلات تشكل النجوم (SFR) ، بالإضافة إلى الخواص الفلكية للزوج ، حيث تبين أن الزوج المجري

*Email: hayder.hussein@sc.uobaghdad.edu.iq

UGC 8335 هوزوج متفاعل يُظهر مؤشرات مهمة على التفاعل ويخضع لعملية دمج. علاوة على ذلك، يتم تصنيف هذا الزوج على أنه زوج مجرات متوسط ويمثل نظامًا فيزيائيًا يتمتع بمعدلات تكوين نجوم متنامية.

الكلمات المفتاحية: المجرات المتفاعلة، المجرات المندمجة، الزوج المجري UGC 8335 E, UGC 8335 W، التحليل الطيفي، اللعان السطحي، فلتر SDSS .

1. Introduction:

It was predicted that there are roughly 2×10^{12} galaxies, considered the fundamental elements of the universe, that have been noticeable within the entirety of the recognized cosmos [1, 2]. The cosmological web, comprising Voids and Filaments, has been constructed the universe. Galaxy groupings and clustering are established at the knots of the grid where the filaments intersect [3]; As a result, the allocation of galaxies in every part of the universe is not identical [4]. Moreover, the presence of this arbitrary distribution increased the likelihood of the emergence and interaction of galaxy pairs. [5].

The present multidimensional redshift surveys of galaxies across the obvious large-scale universe, for example, the SDSS, have effectively revealed the distributions of galaxies in issue [6]. Inspecting galaxy combines and how they interact is crucial for understanding their influence on their morphological characteristics, star-forming rates, evolution, and gravitational affects within galaxies[7, 8]. The technique of surface photometry has been frequently employed in the field of astronomy to quantify the luminosity of galaxies' surfaces; when integrated with spectral analyses, this methodology can yield significant insights into the evolutionary trajectory, morphology, and star-forming propensities of paired galaxies [9, 10]. The analysed pair (UGC 8335 per “The Uppsala General Catalogue of Galaxies (UGC)”) was a galaxy pair composed of two spiral galaxies according to NED.

The left galaxy member of the pair was SDSS J131535.10+620728.4, also referred to as UGC 8335 E, and PGC046114, while the other galaxy of the pair was SDSS J131530.72+620744.8, likewise known as UGC 8335 W, and PGC046133 per; (SDSS), (UGC), and (PGC), respectively, according to both the (NED) and, (HyperLEDA).

The galaxy UGC 8335 E was categorised as interaction (Nair et al., 2010) [11], merger (Lintott et al., 2011) [12], spiral (Sc) (Dobrycheva et al., 2013) [13], and spiral (Sab) with interaction signs (Wieltt et al., 2013) [14]. The galaxy UGC 8335 W was also classified a merger (Lintott et al., 2011) [12], spiral (Sb) with interaction signs (Wieltt et al., 2013) [14]. The principal details of the two galaxies in the pair are presented in Table 1.

Table 1: Principal details pertaining to paired galaxy UGC 8335

Galaxy Name	UGC 8335 E	UGC 8335 W
RA(deg)	198.896 ^a	198.878 ^a
Dec(deg)	62.125 ^a	62.129 ^a
Redshift	0.03078 ^b	0.03134 ^b
Type	Sbc ^c	Sbc ^c
Sub type	Starburst ^b	Star formation ^b
Semi-major axis (kpc)	12.94 ^a	14.45 ^a
Inclination (deg)	82.8 ^c	80.5 ^c
Position Angle (deg)	110.8 ^c	102.6 ^c
Apparent magnitude in the B-band (mag)	13.72 ^c	14.45 ^c

^aNED, ^bSDSS, ^cHyperLEDA

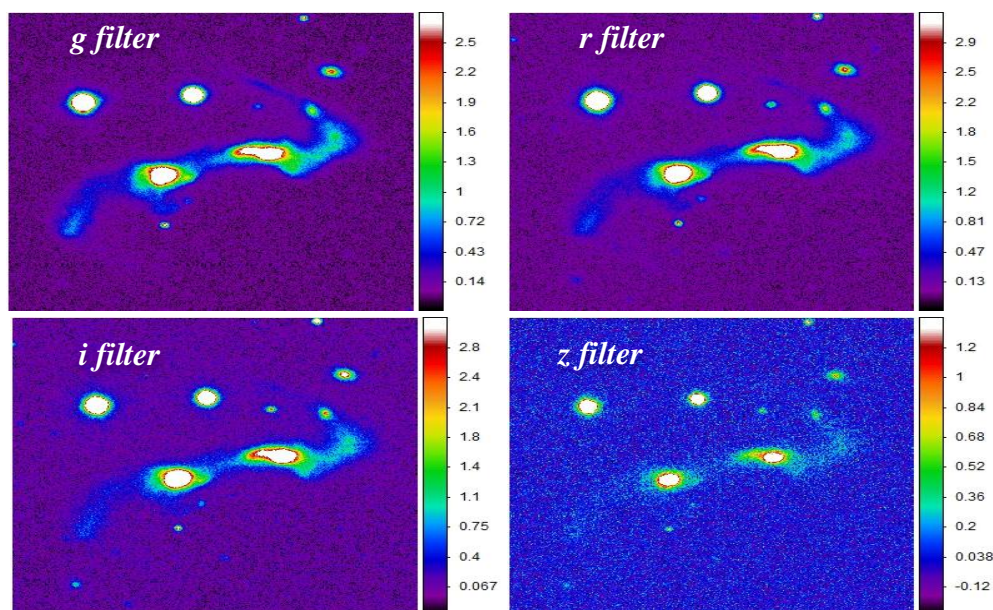


Figure 1: Images of the UGC 8335 pair galaxy in the g,r,i, and z filters.

2. Observations and Reduction of Data

The SDSS provides access to observational data about the two galaxies comprising the pair through its Data Releases (DR7 and DR17) [15, 16], as displayed in Figure 1. The flat and bias field frames for the two galaxies' images were modified using the SDSS pipeline. The isophotes of a pair of galaxies were subjected to ellipse fitting using the ELLIPS function available in the STSDAS Library. The library mentioned above has been implemented into the "Image Reduction and Analysis Facility (IRAF)." The fitting process was conducted across the g, r, i, and z bands. Implementation of the ELLIPS task had the potential to yield isophotal shape variables (B4), intensities (I), accumulative fluxes (f), ellipticities (ϵ), position angles (PA), both vertical and horizontal deviations (x_c, y_c -shift), and ellipticities (ϵ) with the semi-major axes for both galaxies within the UGC 8335 pair. This result directly stems from the application of task. The photometric details facilitated an examination of the interaction and combining conditions of the galaxy pair, as evidenced by the distortions observed in the isophotal properties of the galaxies[8].

The observational data for every image frame of g, r, i, and z filters about the two galaxies of the pair UGC 8335 were subjected to reduction to eliminate the noise sources from the data. The aforementioned task was executed through a series of steps, beginning with eliminating the sky background's intensity values. Subsequently, the frame units were converted from pixels to arcsec^2 . Lastly, the duration of exposure was restricted to 1 s. The values of magnitude (m) have been obtained by using the intensities (I) values that have been subsequently modified for galactic and atmospheric attenuation through Equation 1[17].

$$m = 2.5 \times \log (I \times 10^{(m_0 + k_a + \text{airmass})}) \quad (1)$$

The variables in question are denoted as follows:

- m_0 represents the magnitude of the zero point.
- K_a denotes atmospheric extinction.
- Airmass refers to the airmass associated with the observation of SDSS.

Table 2 displays the g,r,i, and z filter quantities of two galaxies within UGC 8335.

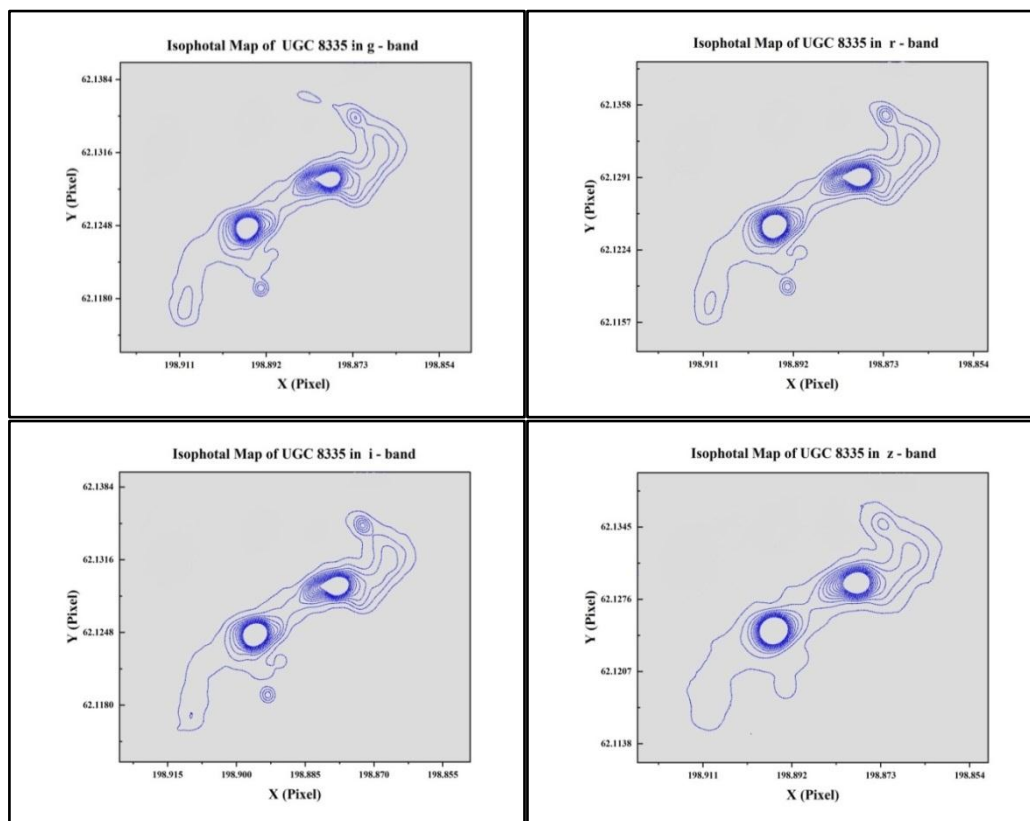
Table 2: Magnitude of zeropoint (m_z), extinction of atmospheric (k_a), and airmass for UGC 8335 [6].

Bands	M_0	K_a	air mass
g	-24.45	0.216	1.161
r	-24.03	0.112	1.158
i	-23.73	0.101	1.159
z	-21.79	0.096	1.160

3. Results and Discussion:

3.1 Morphologies and contour maps of the UGC 8335 galaxy pair

Due to Deep Sky 9 (DS9) analysis, contour maps of the UGC 8335 galaxy pair in g, r, i, and z filters were constructed, as shown in Figure 2. The UGC 8335 E galaxy appeared to have an asymmetric structure that stretched to the west toward the UGC 8335 W galaxy with a bright bulge and two distorted spiral arms extending to the south and southwest of the galaxy, as well as a distinct matter bridge pairing it to the other galaxy component of the pair with a major axis length of roughly 15 kiloparsecs (kpc) at surface brightness levels of 23.89, 23.63, and 23.35 (mag.arcsec^{-2}) in g,r, and i filters. At the same time, it reached 13 kpc at 23.91 (mag.arcsec^{-2}) in the z filter. The UGC 8335 W galaxy has been measured to have a major axis length roughly 16 kpc with surface brightness levels of 23.89, 23.63, and 23.35 in g, r, and i filters, while it reached around 14 kpc at 23.91 (mag.arcsec^{-2}) in the z band. It had a bright bulge surrounding an asymmetric disk arrangement that stretched to the east toward the UGC 8335 E galaxy, a deformed spiral arm that extended north-west from the galaxy, and a distinct bridge of matter connecting with the other galaxy member of the pair. Table 3 shows the surface brightness levels of the UGC 8335 galaxy pair's the g, r, i, and z outer isophotes.

**Figure 2:** Contour maps of UGC 8335 pair in g, r, i, and z filters

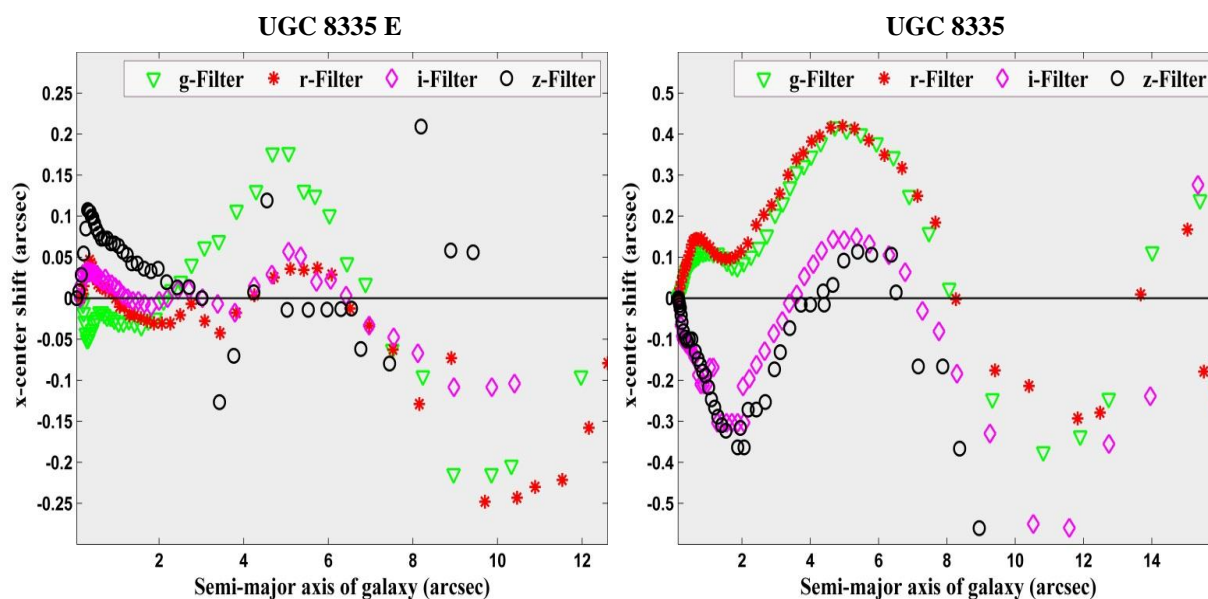


Figure 3: The x centre shifts (x_c) as functions of the semi major axis of the two galaxies UGC8335 E (left) and W (right)

Table 3: UGC8335 brightness levels of the outer isophotes

Galaxy	Bands	Magnitude (mag)	Surface brightness (mag.arcsec ⁻²)	Step
UGC 8335	g	25.99	23.98	0.255
	r	25.64	23.63	0.255
	i	25.36	23.35	0.255
	z	25.92	23.91	0.052

3.2 The UGC 8335 Galaxy Pair's Center Shifts

The parameters (x_c , y_c) shown in Figures 3 and 4 describe the deviations of the centres of both galaxies in the UGC 8335 galaxy pair as observed through the g, r, i, and z bands.

The x_c of UGC 8335 E showed some stability from the centre to roughly 1.4 kpc (2 arcsec), then increased considerably to the north toward the bridge connecting the two members of the pair and consequently toward UGC 8335 W, especially in the g band, with a deviance value approaching 0.12 kpc (0.2 arcsec); The x_c thereafter declined to the south toward the arms at roughly 5 kpc (8 arcsec) and continued to the galaxy's borders, with variance levels ranging between 0.07 and 0.13 kpc (0.1 and 0.2 arcsec) in the g, r and i bands.

Nonetheless, the x_c of UGC 8335 W fluctuated in the inner region until about 1.4 kpc (2 arcsec) from the centre, then rose significantly to the north toward the arm in all bands, with a deviance value reaching 0.3 kpc (0.4 arcsec); Within about 5 and 8.5 kpc (8 and 13 arcsec), the x_c dropped to the south toward the bridge that connects the two components of the pair and, ultimately, toward UGC 8335 E, with variation values ranging between 0.2 and 0.35 kpc (0.3 and 0.6 arcsec) in the g, r and i bands; Afterwards, it returned to fluctuating at the outermost edges of the g, r and i bands as a result of the combined effects of the arm and the paired galaxy UGC 8335 E and the bridge.

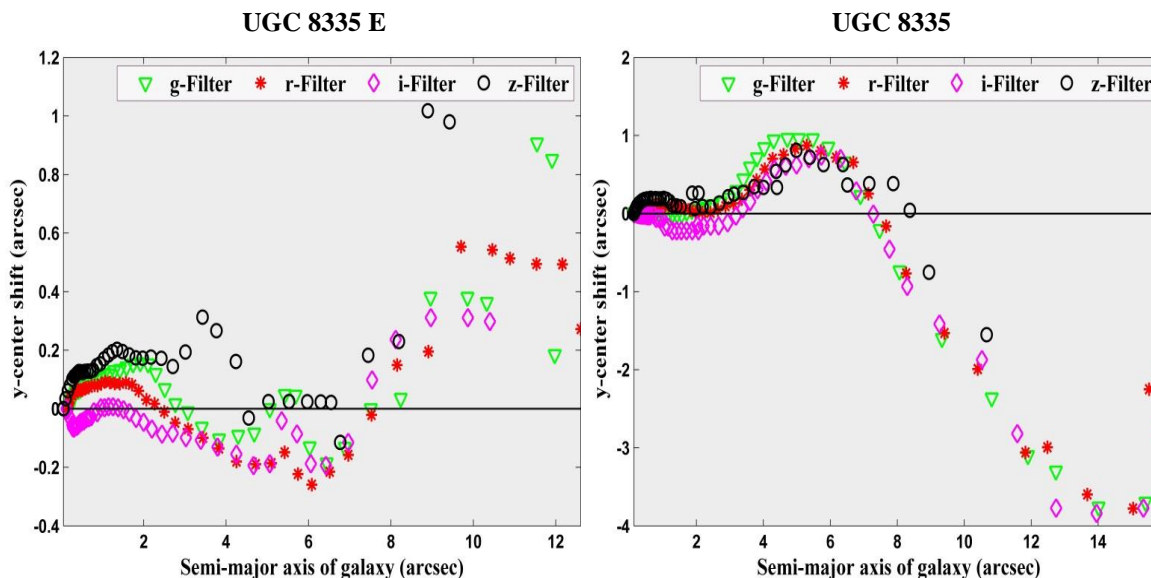


Figure 4: The y_c centre shifts (y_c) as functions of the semi major axis of the two galaxies UGC8335 E (left) and W (right)

The y_c of UGC 8335 E exhibited a degree of uniformity from center to approximately 1.4 kpc (2 arcsec). Subsequently, it shifted slightly to the west toward the bridge that links the two galaxies in the pair and thus to UGC 8335 W in the g, r, and i bands, leading to variance values ranging between 0.13 and 0.2 kpc (0.2 and 0.3 arcsec). The y_c subsequently climbed to the east toward the arms at around 5 kpc (8 arcsec) and remained until the galaxy's boundaries, with deviation levels in the i, r, and g bands of 0.2, 0.4, and 0.6 kpc (0.3, 0.6 and 0.9 arcsec), respectively.

The y_c of UGC 8335 W demonstrated a certain consistency from the centre to approximately 1.4 kpc (2 arcsec). Afterwards, the deviation value reached 0.65 kpc (1 arcsec) as it increased considerably to the east toward the bridge that joins the two members of the pair and then eventually toward UGC 8335 E in all bands. At close to 5 kpc, the y_c began to decline to the west toward the arm until the outer borders, with shift readings above 2.5 kpc (4 arcsec) in the g, r and i bands.

3.3 The UGC 8335 Galaxy Pair's Position Angles

The Position Angles (PA) within the bulge of the UGC 8335 E galaxy exhibited irregularity until reaching a distance of approximately 1.4 kpc (2 arcsec). Subsequently, a reduction in position angle (PA) was observed along the semi-major axis up to approximately 2.6 kpc (4 arcsec), with a range of variation of 8° across all bands. However, a sudden increase in PA was noted from approximately 2.6 to 5 kpc (2 to 8 arcsec), with approximately 20° observed across all

bands. On the other hand, beyond a distance of 5 kpc (8 arcsec), the position angle tended to decrease, with recorded shift values ranging from 16° to 22° in the g, r, and i filters.

In different phrases, UGC 8335 E underwent a tilt toward the north, specifically by 8 degrees in the direction of UGC 8335 W. Subsequently, it encountered a convoluted movement in the southern direction, with a deviation of 20 degrees from the galaxy UGC 8335 W. Eventually, it returned to drifting toward the north, with a range of deviance between 16 and 22 degrees, due to the distortion of galaxy shape produced by the interaction between the pair's constituent galaxies.

The UGC 8335 W exhibited notable variations in its Position Angles (PA) within the inner region up to approximately 1.4 kpc (2 arcsec) from the central region across all bands. Then, the PA increased from approximately 90° to 106° and remained relatively stable until approximately 7.5 kpc (12 arcsec) across all bands. Beyond this point, the PA decreased from roughly 106° to 83° degrees until the edges of the galaxy across all bands; The galaxy indicates an abnormal tendency to shift in the southern direction, specifically towards the bridge that links the two galaxies of the pair, and eventually toward UGC 8335 E at an angle of approximately 16° . Likewise, it tends to shift in the northern direction, away from UGC 8335 E, toward the arm at an angle of roughly 23° , as illustrated in Figure 5.

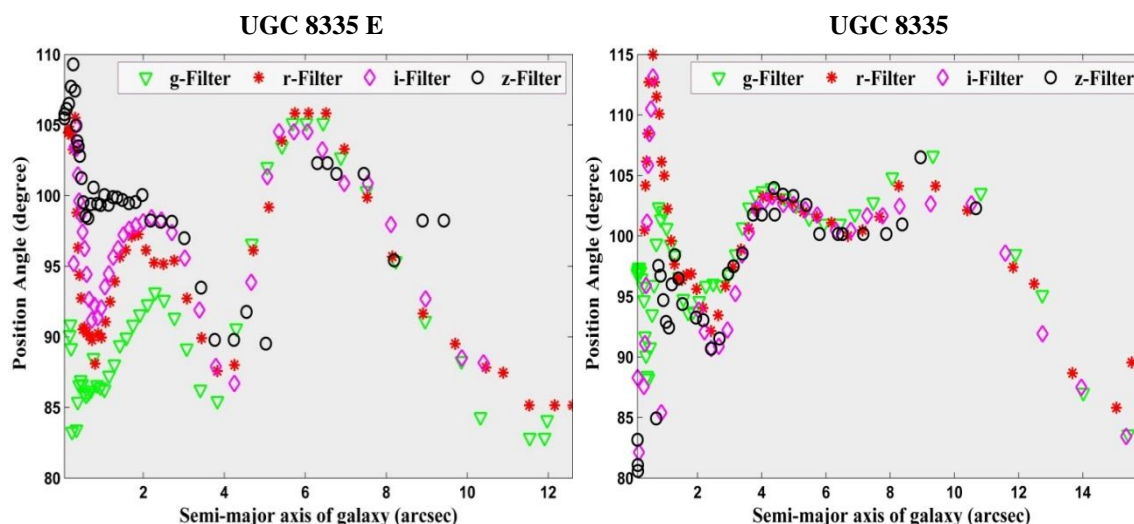


Figure 5: The position angles (PA) as functions of the semi major axis of the two galaxies UGC8335 E (left) and W (right)

3.4 UGC 8335 Galaxy Pair's Ellipticities

The investigation noticed fluctuations in the ellipticity (ϵ) of UGC 8335 E within the g, r, i, and z bands in its central regions up to a distance of approximately 1.4 kpc (2 arcsec). Next, a

significant reduction in ellipticity was noted up to a separation of approximately 3 kpc. Beyond that, the ellipticity continually rose toward the farthest ends of the galaxy within all bands. The mid regions of the galaxy experienced a decrease in flatness, whereas the outer regions experienced an increase in flatness. In addition, the UGC 8335 W galaxy exhibited oscillations in ellipticity across the g, r, i, and z bands within a bulge until approximately 1.4 kpc (2 arcsec). Subsequently, the E value gradually increased along the semi-major axis until just over 5 kpc (8 arcsec) in the g, r, and z filters, followed by a slight decrease until the outer edges; this suggests that the middle portions of the galaxy appeared flatter than the outer regions. This asymmetry arises due to the distortions of the galaxies' form owing to the interaction between the component galaxies of a pair, as shown in Figure 6.

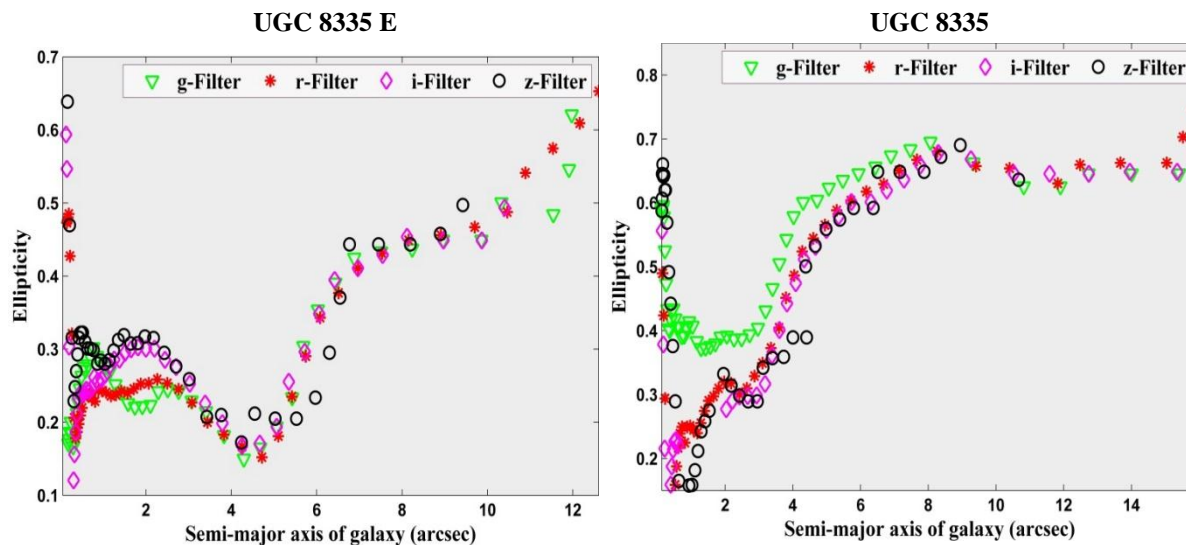


Figure 6: The ellipticity (ϵ) as functions of the semi major axis of the two galaxies UGC8335 E (left) and W (right)

3.5 The shape parameter (B_4) of UGC 8335 Pair

The galaxy UGC 8335 E exhibits a discernible variation in the shape parameter (B_4) from its ellipse shape, characterized by a significant fluctuation in the bulge region, followed by a phase of relative constancy with values close to zero, extending up to a radial length of approximately 3 kpc. Following this, a discernible peak emerges with a radius of approximately 4 kpc from the galaxy center, followed by a subsequent decrease in B_4 levels until reaching approximately six kpc (9 arcsec) across all bands. The abovementioned decrement is followed by clear upward shifts that persist until the outer edges of the g, r and i spectral bands.

The galaxy UGC 8335 W exhibits irregularity B_4 values from the bulge up to a distance of approximately 1.4 kpc (2 arcsec), followed by a narrow region of relative stability that extends to approximately 2 kpc. Additionally, there is a distinct peak centered at nearly 2.7 kpc (4.3 arcsec). Next, B_4 drops to around 6 kpc (9 arcsec) in all bands, followed by evident shifts in the positive direction that extend to the outside edges in the g,r,and i filters, while the z filter did not get a clear condition due to the high distortion.

The apparent fluctuations observed in the mid-regions and the edges of the two galaxies in the pair, as revealed in all filters, suggest UGC 8335 E and W galaxies have undergone evident distortion due to the interaction between them, as can be seen in Figure 7.

3.6 Magnitudes of the UGC 8335 Galaxy Pair

The UGC 8335 E galaxy demonstrated acceptable magnitude values across all bands, with a tendency to decrease from its center to its periphery, except for inconsistent behavior observed at just under 4 - 4.5 kpc (4.5 to 7 arcsec) in all bands. On the other hand, the magnitudes of the UGC 8335 W galaxy likewise showed an identical pattern, diminishing along the semimajor axis from the galactic center toward the galaxy borders in all bands, except for a few g, r, and i band variabilities close to the edges, as shown in Fig. 8.

Equation 1 was used to determine the total apparent magnitudes of the two galaxies in the UGC 8335 pair based on cumulative flux data with applied corrected values from Table 2 .

Table 4 presents the apparent magnitudes (m) in the g,r,i, and z bands obtained through calculations, along with the corresponding SDSS apparent magnitudes.

Table 4: UGC8335 apparent magnitudes (calculated, selected from SDSS) in the g, r, i, and z filters

Galaxy	Our work				SDSS			
	(m _g)	(m _r)	(m _i)	(m _z)	(m _g)	(m _r)	(m _i)	(m _z)
UGC 8335 E	15.03	14.55	14.33	14.13	15.08	14.61	14.30	13.98
UGC 8335 W	14.95	14.51	14.20	14.27	15.17	14.61	14.19	13.94

3.7 UGC 8335 Paired Galaxy Astrometric Results

Upon Hubble’s law implementation, Equation (2) was used to determine the mean distance (D_a) of the paired galaxy, measured in megaparsecs (Mpc)[18].

$$D_a = \frac{c z_a}{H_0} \tag{2}$$

where H₀ denotes the Hubble constant with a value of (70 km/s .Mpc), z_a represents the average redshift, computed as (z_a= z₁+z₂/ 2), and c signifies the velocity of light[19].

Karachentsev’s Equation has been applied to identify the distance that separates the two galaxies in the pair (d_{sep}) in kpc [20].

$$d_{sep} = \theta_{12} D_a \tag{3}$$

The two galaxies separated by an angle denoted as θ₁₂ in degree. The subsequent Equation was used to derive the relative velocity (v_r) of both galaxies[20].

$$v_r = \sqrt{(cz_1 - cz_2)^2} \tag{4}$$

The next equation can be employed to determine the combined orbital mass of the two galaxies in the pair (M_p) with respect to the mass of the Sun (M_⊙)[20].

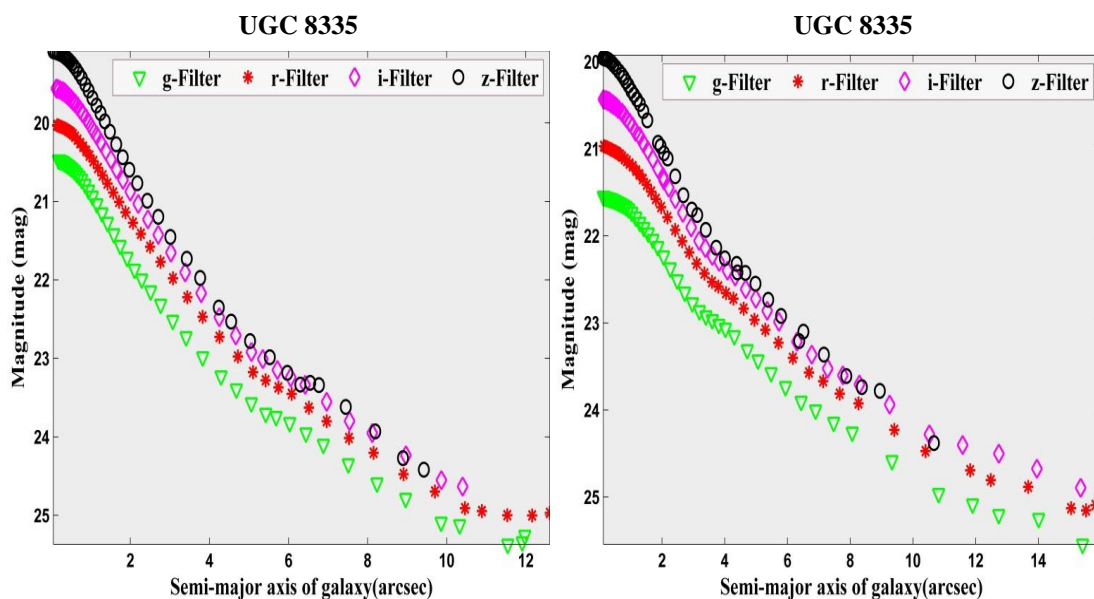


Figure 8: Magnitude as functions of the semi major axis of the two galaxies UGC8335 E (left) and W (right)

$$M_p = 3.4 \frac{d_{\text{sep}} v_r^2}{G} \quad (5)$$

where G: The constant denoting the force of gravity, Table 5 demonstrates the results of the aforementioned computations.

Table 5: UGC 8335 Paired Galaxy Astrometric results

$D_a(\text{Mpc})$	$d_{\text{sep}}(\text{kps})$	$v_r(\text{km.s}^{-1})$	$M_p(M_\odot)$
133.14	43.68	167.7	9.64×10^{11}

The measurements of the cumulative flux data for both galaxies in the UGC 8335 pair can be employed to derive the total luminosity of the pair as a hole (L_G), total absolute magnitude (M_G), and total apparent magnitude m_G regarding the solar luminosity (L_\odot) for g, r, i, and z filters, respectively, by using Eq.s. (1), (6), and (7); consequently, the mass-to-light ratio (M_p/L_G) can be computed for the same filters, as shown in Table 6[21-23].

$$m_G - M_G = 5 \times \log \left(\frac{D_a(\text{Mpc})}{10} \right) \quad (6)$$

$$M_G - M_{(g,r,i,\text{and } z)\odot} = 2.5 \times \log \left(\frac{L_\odot}{L_G} \right) \quad (7)$$

The notation $M_{(g)\odot}$, $M_{(r)\odot}$, $M_{(i)\odot}$, $M_{(z)\odot}$ is utilized to represent the absolute magnitude of the sun in accordance with the Vega system [24].

Table 6: UGC 8335 Apparent magnitude (m_G), absolute magnitude (M_G), luminosity (L_G), and mass -to-light ratio

Filters	$m_G \text{ mag}$	$M_G \text{ mag}$	$L_G (L_\odot)$	$M_p/ L_G (M_\odot/L_\odot)$
g	14.24	-21.38	4.42×10^{10}	21.79
r	13.78	-21.84	3.54×10^{10}	27.26
i	13.51	-22.11	3.31×10^{10}	29.13
z	13.45	-22.17	2.97×10^{10}	32.46

3.8 The UGC 8335 Galaxy Pair Spectra and Star Formation Rates

The spectra of the UGC 8335 E and the UGC 8335 W galaxies exhibited noteworthy lines of emissions of OII, SII, OIII, NII, H β , and H α , as illustrated in both Figures 9 and 10. The luminosity of the OII (F) in the UGC 8335 E and W galaxies spectra can be utilized to evaluate their star-forming rates (SFR) because the luminosity of the OII emission lines is typically contingent on ionizing photons, as per Equations 8 and 9 [25, 26]:

$$\text{SFR} (M_\odot/\text{year}) = \frac{F}{3 \times 10^{33} \text{ erg/s}} \quad (8)$$

$$F = 4 \times \pi \times D_L \times S_{\text{OII}} \text{ erg/s} \quad (9)$$

whereas is D_L is the luminosity distance, and S_{OII} Flux of OII, the results are presented in

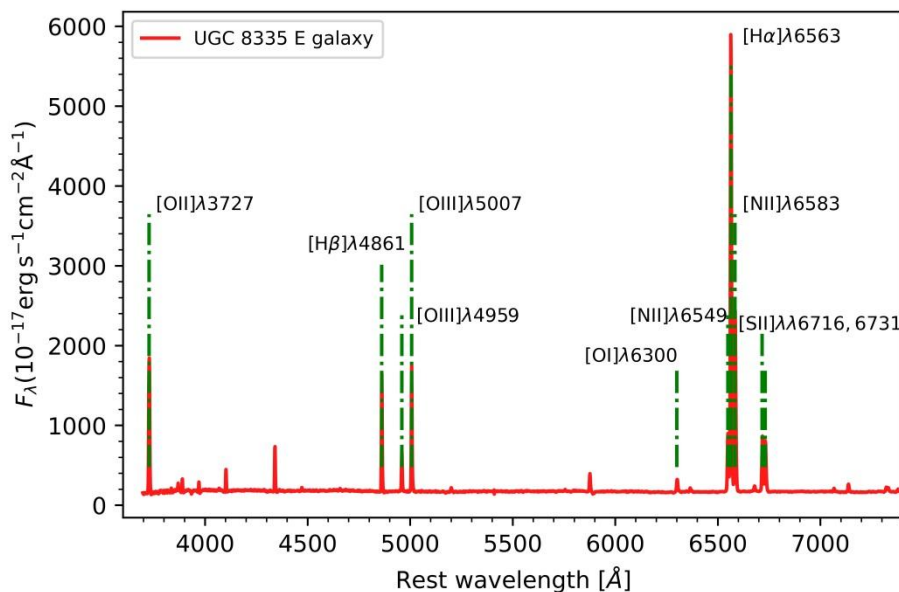


Figure .9 The UGC 8335 E galaxy's spectra

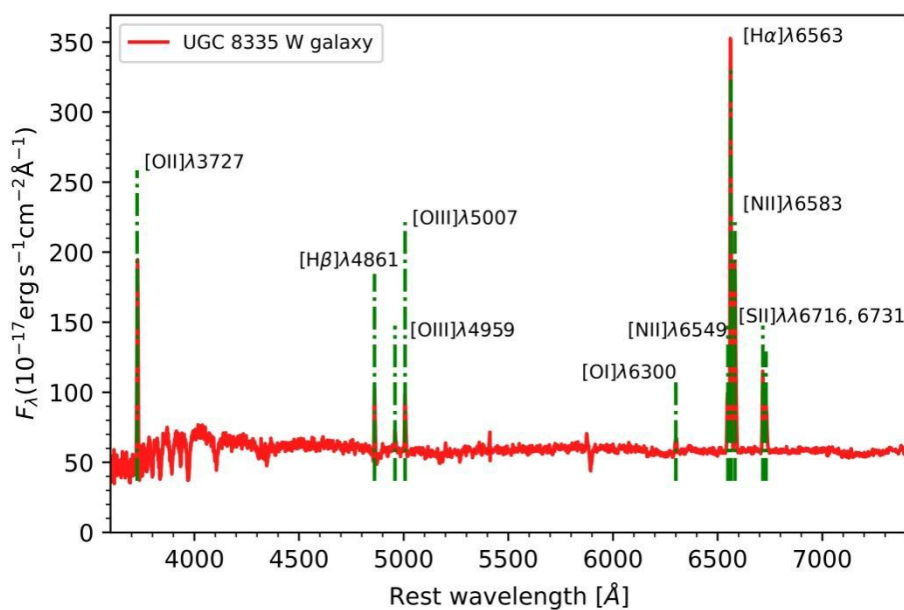


Figure 10: The UGC 8335 W galaxy's spectra

Table 7: The UGC 8335 galaxy pair ' estimated SFR, distance, redshift, and flux

Galaxy	$S_{\text{OII}} (10^{-17} \text{ erg.s}^{-1}.\text{cm}^{-2})$	z	$D_L \text{Mpc}$	$\text{SFR} (M_{\odot}.\text{Yr}^{-1})$
UGC 8335 E	5910.8	0.030	131.4	4.11
UGC 8335 W	571.8	0.031	135.9	0.43

4. Conclusions:

a) On the basis of the photometric results, it can be inferred that the UGC 8335 galaxy pair appears to be an interacting pair of galaxies with strong interaction signs undergoing a merging process, where the contour maps of both galaxies in the UGC 8335 pair exhibit an asymmetric stretched structure and distorted spiral arms. Additionally, a discernible matter bridge connects the two galaxies in the pair; Identifiable centers shifts of UGC 8335 E and

W, one toward the other galaxy in the pair; The galaxies UGC 8335 E and UGC 8335 W exhibit multiple tilts in both the northern and southern directions; There is an asymmetry in the ellipticity values of the UGC 8335 E, W galaxies; the shape parameters (B4) of the UGC 8335 E, W galaxies suggest that the two galaxies have undergone evident distortion; There are few variabilities in the values of magnitudes of the UGC 8335 E, W galaxies; These signs appear due to the distortions of the galaxies' forms owing to the interaction between them. The results of our investigation closely agree with those of (Nair et al., 2010)[11], (Lintott et al., 2011)[12], and (Wieltt et al., 2013)[14].

b) The UGC 8335 galaxy pair meets Patton's criteria [27] for being an intermediate galaxy pair with a spacing of 43.68 kpc and a relative velocity of 167.7 km/s.

c) The UGC 8335 mass light ratio was determined to be nearly 21.79, 27.26, 29.13, and 32.46 (M_{\odot}/L_{\odot}) in all filters. This finding confirms that the UGC 8335 pair is a physical system that agrees with Karachentsev's thought [20].

d) The star-forming ratios (SFRs) of both galaxies, UGC 8335 E and W, were computed to be 4.11 and 0.43 M_{\odot}/Year , respectively.

Understanding the history, structure, and development of the universe requires valuing the primary structural components. The results of our study are crucial in this continuation.

References

- [1] M. Abd Elaziz, K.M. Hosny, and I. Selim, "Galaxies image classification using artificial bee colony based on orthogonal Gegenbauer moments," *Soft Computing*, vol. 23, pp. 9573-9583, 2019.
- [2] M.Y. Marov, "The Structure of the Universe," in *The Fundamentals of Modern Astrophysics*: Springer, 2015, pp. 279-294.
- [3] R.J. Van Weeren, F. Andrade-Santos, W.A. Dawson, N. Golovich, D.V. Lal, H. Kang, D. Ryu, M. Brüggén, G.A. Ogrean, and W.R. Forman, "The case for electron re-acceleration at galaxy cluster shocks," *Nature Astronomy*, vol. 1, no. 1, pp. 1-6, 2017.
- [4] M. Argudo-Fernández, S. Verley, G. Bergond, S.D. Puertas, E.R. Carmona, J. Sabater, M.F. Lorenzo, D. Espada, J. Sulentic, and J. Ruiz, "Catalogues of isolated galaxies, isolated pairs, and isolated triplets in the local Universe," *Astronomy & Astrophysics*, vol. 578, p. A110, 2015.
- [5] A. Das, B. Pandey, S. Sarkar, and A. Dutta, "Galaxy interactions in different environments: An analysis of galaxy pairs from the SDSS," *arXiv preprint arXiv:2108.05874*, 2021.
- [6] A. Almeida, S.F. Anderson, M. Argudo-Fernández, C. Badenes, K. Barger, J.K. Barrera-Ballesteros, C.F. Bender, E. Benitez, F. Besser, and D. Bizyaev, "The Eighteenth Data Release of the Sloan Digital Sky Surveys: Targeting and First Spectra from SDSS-V," *arXiv preprint arXiv:2301.07688*, 2023.
- [7] J.H. Knapen, M. Cisternas, and M. Querejeta, "Interacting galaxies in the nearby Universe: only moderate increase of star formation," *Monthly Notices of the Royal Astronomical Society*, vol. 454, no. 2, pp. 1742-1750, 2015.
- [8] Y.M. Hendy, "BVR photometric investigation of galaxy pair KPG 562," *NRIAG Journal of Astronomy and Geophysics*, vol. 7, no. 1, pp. 4-9, 2018.
- [9] X. Pan, H. Lu, S. Komossa, D. Xu, W. Yuan, L. Sun, P.S. Smith, S. Zhang, P. Jiang, and C. Yang, "A Deeply Buried Narrow-line Seyfert 1 Nucleus Uncovered in Scattered Light," *The Astrophysical Journal*, vol. 870, no. 2, p. 75, 2019.
- [10] H.R. Al-baqir, A.K. Ahmed, and D. Gamal, "Surface Photometry of NGC 3 Lenticular Galaxy," *Iraqi Journal of Science*, pp. 2080-2086, 2019.
- [11] P.B. Nair and R.G. Abraham, "A catalog of detailed visual morphological classifications for 14,034 galaxies in the sloan digital sky survey," *The Astrophysical Journal Supplement Series*, vol. 186, no. 2, p. 427, 2010.
- [12] C. Lintott, K. Schawinski, S. Bamford, A. Slosar, K. Land, D. Thomas, E. Edmondson, K. Masters, R.C. Nichol, and M.J. Raddick, "Galaxy Zoo 1: data release of morphological classifications for nearly 900 000 galaxies," *Monthly Notices of the Royal Astronomical Society*, vol. 410, no. 1, pp. 166-178, 2011.

- [13] D. Dobrycheva, "The new galaxy sample from SDSS DR9 at $0.003 \leq z \leq 0.1$," *Odessa Astronomical Publications*, vol. 26, no. 2, pp. 187-189, 2013.
- [14] K.W. Willett, C.J. Lintott, S.P. Bamford, K.L. Masters, B.D. Simmons, K.R. Casteels, E.M. Edmondson, L.F. Fortson, S. Kaviraj, and W.C. Keel, "Galaxy Zoo 2: detailed morphological classifications for 304 122 galaxies from the Sloan Digital Sky Survey," *Monthly Notices of the Royal Astronomical Society*, vol. 435, no. 4, pp. 2835-2860, 2013.
- [15] D.G. York, J. Adelman, J.E. Anderson Jr, S.F. Anderson, J. Annis, N.A. Bahcall, J. Bakken, R. Barkhouser, S. Bastian, and E. Berman, "The sloan digital sky survey: Technical summary," *The Astronomical Journal*, vol. 120, no. 3, p. 1579, 2000.
- [16] N. Abdurro'uf, K. Accetta, C. Aerts, V. Silva Aguirre, R. Ahumada, N. Ajgaonkar, N. Filiz Ak, S. Alam, C. Allende Prieto, and A. Almeida, "The Seventeenth Data Release of the Sloan Digital Sky Surveys: Complete Release of MaNGA, MaStar, and APOGEE-2 Data," *The Astrophysical Journal. Supplement Series*, vol. 259, no. 2, 2022.
- [17] A.K. Ahmed, "Comparison of the Structure of Spiral and Lenticular Galaxies, NGC 4305 and NGC 4203 as a Sample: Astronomy And Space Department, College of Sciences, University of Baghdad, Baghdad, Iraq," *Iraqi Journal of Science*, pp. 2051-2059, 2023.
- [18] Y.E. Rashed, M.N. Al Najm, and H.H. Al Dahlaki, "Studying the Flux Density of Bright Active Galaxies at Different Spectral Bands," *Baghdad Science Journal*, vol. 16, no. 1 Supplement, 2019.
- [19] Y.E. Rashed, A. Eckart, M. Valencia-S, M. Garcia-Marin, G. Busch, J. Zuther, M. Horrobin, and H. Zhou, "Line and continuum variability in active galaxies," *Monthly Notices of the Royal Astronomical Society*, vol. 454, no. 3, pp. 2918-2945, 2015.
- [20] I.d. Karachentsev, "Double galaxies," *Moscow Izdatel Nauka*, January 01, 1987 1987.
- [21] Z. Adnan and A.K. Ahmed, "Surface Photometry of Spiral Galaxy NGC 5005 and Elliptical Galaxy NGC 4278," *Baghdad Science Journal*, vol. 15, no. 3, 2018.
- [22] C. Barbieri and I. Bertini, *Fundamentals of astronomy*. CRC Press, 2020.
- [23] S.A.A. Albakri, M.N.A. Hussien, and H. Herdan, "Measurement of the distance to the central stars of Nebulae by using Expansion methods with Alladin Sky Atlas," in *IOP Conference Series: Materials Science and Engineering*, 2020, vol. 757, no. 1: IOP Publishing, p. 012043, doi: 10.1088/1757-899X/757/1/012043.
- [24] C.N. Willmer, "The absolute magnitude of the sun in several filters," *The Astrophysical Journal Supplement Series*, vol. 236, no. 2, p. 47, 2018.
- [25] S.H. Kareem and Y.E. Rashed, "Studying the Correlation between Supermassive Black Holes and Star Formation Rate for Samples of Seyfert Galaxies (Type 1 and 2)," *Iraqi Journal of Physics*, vol. 19, no. 48, pp. 52-65, 2021.
- [26] Y.E. Rashed, J. Zuther, A. Eckart, G. Busch, M. Valencia-S, M. Vitale, S. Britzen, and T. Muxlow, "High-resolution observations of SDSS J080800. 99+ 483807.7 in the optical and radio domains-A possible example of jet-triggered star formation," *Astronomy & Astrophysics*, vol. 558, p. A5, 2013.
- [27] D.R. Patton, S.L. Ellison, L. Simard, A.W. McConnachie, and J.T. Mendel, "Galaxy pairs in the Sloan Digital Sky Survey–III. Evidence of induced star formation from optical colours," *Monthly Notices of the Royal Astronomical Society*, vol. 412, no. 1, pp. 591-606, 2011.